# Role of Asn-16 and Ser-19 in Anthopleurin B Binding. Implications for the Electrostatic Nature of $Na_V$ Site 3[†,‡]

Anna L. Seibert,[§] Jinrong Liu,[||] Dorothy A. Hanck,[||] and Kenneth M. Blumenthal*[,§]

*Department of Biochemistry, State University of New York at Buffalo, Buffalo, New York 14214, and Departments of Medicine, Pharmacological, and Physiological Sciences, University of Chicago, Chicago, Illinois 60637*

*Received February 25, 2004; Revised Manuscript Received April 5, 2004*

ABSTRACT: Anthopleurin B (ApB) is a type 1 sea anemone toxin, which binds to voltage-sensitive sodium channels ($Na_V$'s), thereby delaying channel inactivation. Previous work from our laboratories has demonstrated that the structurally unconstrained region involving residues 8−17 of this polypeptide, designated the Arg-14 loop, is important for full toxin affinity (Seibert et al., (2003) *Biochemistry 42*, 14515). Within this region, important contributions are made by residues Arg-12 and Leu-18 (Gallagher and Blumenthal, (1994) *J. Biol. Chem. 269*, 254; Dias-Kadambi et al., (1996) *J. Biol. Chem. 271*, 23828). Moreover, replacement of glycine residues found at positions 10 or 15 of the loop by alanine has been shown to have profound, isoform-selective effects on toxin-binding kinetics (Seibert et al., (2003) *Biochemistry 42*, 14515). To thoroughly understand the importance of this entire region, the work described here investigates the contribution of ApB residues Asn-16, Thr-17, and Ser-19 to toxin affinity and isoform selectivity. Our results demonstrate that residues within and proximal to the C terminus of the Arg-14 loop are important modulators of ApB affinity for $Na_V$ channels, indicating that the loop and channel site 3 are likely in close contact. A comparison of the effects of multiple replacements at each position reveals that Asn-16 and Ser-19 are involved in binding, whereas Thr-17 is not. The fact that anionic replacements for Asn-16 or Ser-19 are highly deleterious for toxin binding strongly suggests that site 3 contains either formal anionic residues or regions of high electron density, which could be formed by aromatic clusters. These data represent the first indication of the presence of such residues or regions within $Na_V$ site 3.

Type one sea anemone toxins, exemplified by Anthopleurin B (ApB)[1] (*1*), compete with α-scorpion toxins for binding to site 3 of voltage-sensitive sodium channels ($Na_V$'s) (*2*−*6*). Although structurally unrelated (*6*−*8*), α-scorpion and anemone toxins exhibit nearly identical physiologic effects. When analyzed by whole-cell patch clamp, bound toxin allows current to continue to flow at times far beyond the point at which channels not modified by toxin have inactivated. This effect is due to a delay in channel inactivation secondary to inhibition of the movement of the voltage sensor in domain IV (*9*−*12*). Previous work from our laboratories has determined that a key binding interaction between Lys-37 of ApB and Asp-1612, a residue in the $D_{IV}$ S3−S4 linker of the rat cardiac isoform $Na_V1.5$, contributes ∼1.5 kcal toward formation of the complex (*13*). This residue is homologous to Glu-1613 of rat neuronal isoform $Na_V1.2$, which has been shown to interact with the α-scorpion toxin LqqV and the type 1 sea anemone toxin AS-II (*14*). These interactions clearly establish the involvement of the classically defined domain IV S4 region in the binding site of these toxins. This region has also been linked genetically to diseases characterized by aberrant inactivation kinetics (*15*).

ApB is a 49-residue polypeptide neurotoxin isolated from the sea anemone *Anthopleura xanthgrammica*. Like many other ion-channel toxins, ApB contains a high density of disulfide bonds (three) and is dominated by *β* structure (*16*−*19*). Curiously, all type 1 anemone toxin structures (*7*, *16*, *20*) lack medium- and long-range constraints for residues 8−17 (ApB numbering), leaving this region poorly defined in their calculated structures (Figure 1). We have previously shown that conversion of either Gly-10 or Gly-15 to alanine greatly diminishes toxin affinity, especially to $Na_V1.2$, suggesting that the inherent flexibility of this toxin region may play an essential, isoform-dependent role in binding (*21*). In addition, Arg-12 and Leu-18, which are located within and adjacent to this flexible loop, contribute significantly to the tight affinity of ApB for $Na_V$ channels (*22*, *23*), while Asp-9, Pro-13, and Arg-14 do not (*24*−*26*). To more completely explore functional correlates of the loop region, we report here the contribution of ApB residues Asn-16, Thr-17, and Ser-19 to channel affinity and isoform selectivity.

## MATERIALS AND METHODS

*Reagents and Enzymes.* The highest grades of commercially available enzymes and chemicals were used for

* To whom correspondence should be addressed. E-mail: kblumen@buffalo.edu. Phone: 716-829-2727. Fax: 716-829-2725.

[†] This work was supported by Grant GM-60582 (to K.M.B. and D.A.H.) from the National Institute of Health and AHA0110113T (to A.L.S.) from the American Heart Association.

[||] Portions of this work have been presented in abstract format in *FASEB J.*, 2000 and *Biophys. J.*, 2003.

[‡] State University of New York at Buffalo.

[§] University of Chicago.

[1] Abbreviations: Wt-ApB, wild-type Anthopleurin B; $Na_V$, voltage-sensitive sodium channel; LqqV, purified *Leiurus quinquestriatus quinquestriatus* toxin V; AS II, *Anemonia sulcata* toxin II.

10.1021/bi0496135 CCC: $27.50 
Published on Web 05/07/2004

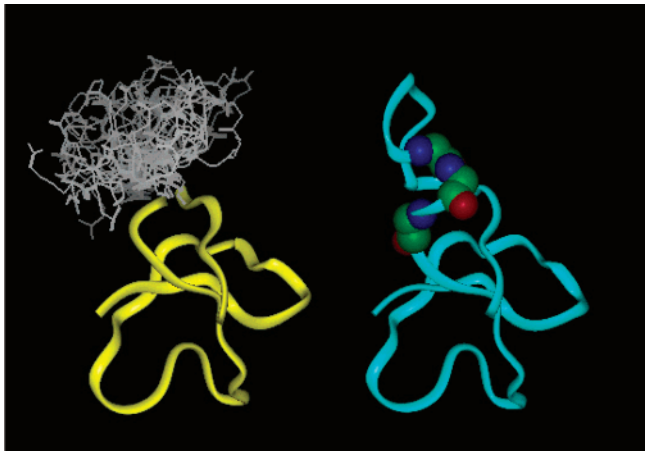

FIGURE 1: Solution structure of ApB. The left panel depicts the 20 individual backbone structures calculated by Monks et al. (*16*). The well-structured region of the molecule (residues 1−7 and 18−49) is represented by the yellow ribbon, while the backbone conformation of each individual structure is shown in white for the Arg-14 loop. The averaged structure is shown on the right, with the residues targeted in the present paper shown in CPK format and colored by atom.

all experiments. General chemicals were purchased from Sigma−Aldrich (St. Louis, MO), while Staphylococcal V8 protease was purchased from ICN (Costa Mesa, CA). Cell culture products, restriction enzymes, and isopropyl-$\beta$-D-thiogalactopyranoside were purchased from Invitrogen Life Technologies, Inc. (Carlsbad, CA).

*Cell Culture.* To analyze the effects of ApB on the human cardiac voltage-sensitive sodium channel, cDNA encoding human $Na_V1.5$ was cloned into plasmid $pRcCMV_{II}$ and stable cell lines were constructed in HEK-293 cells using neomycin selection. These cells were grown in low glucose Dulbecco's modified Eagle's medium (DMEM) supplemented with 10% fetal bovine serum (FBS), 1% penicillin−streptomycin, and 200 $\mu$g/mL G418 in 5% $CO_2$. The murine neuroblastoma cell line, N1E-115 was obtained from ATCC (Manassas, VA) and was used to study the effects of ApB on $Na_V1.2$ (*27*, *28*). N1E-115 cells were grown in high glucose DMEM supplemented with 10% FBS and 1% penicillin−streptomycin in 5% $CO_2$. To prepare both cell lines for study, they were trypsinized, centrifuged, resuspended in media, and then either placed on coverslips and returned to the incubator for use later that day or placed directly into the cell chamber for immediate analysis.

*Molecular Biology.* Site-directed mutagenesis was performed using the QuikChange system (Stratagene, La Jolla, CA) in the recombinant plasmid pKB13, previously described by our laboratory (14), or in the pKB13-derived plasmids, pJL2 and pJL5. The latter two plasmids are identical to pKB13 except that the sequence encoding the pentaglutamyl linker fusing ApB to the C-terminal end of the bacteriophage T7 gene 9 was changed to encode KGEEM for pJL2 or shortened to a single glutamate for pJL5. Nucleotide sequences of all derived plasmids were validated by the dideoxy method to ensure that the correct product was encoded. All variant proteins will be referred to by the single letter abbreviation of the wt-ApB amino acid followed by its position number and the single letter abbreviation for the replacement amino acid. The mutagenesis yielded the plasmids (and encoded proteins) pAE1 (N16D), pAS12 (N16A), pAS13 (S19A), pAS14 (S19D), pAS15 (T17A), pAS30 (T17D), pDaM808 (S19R), and pSA2 (N16R).

*Protein Purification and Analytical Methods.* ApB and all variants were expressed in *Escherichia coli* BL21(DE3) as fusion proteins under control of the T7 promoter. After purification of the fusion protein by anion-exchange chromatography, disulfide pairs were oxidized in the presence of a glutathione redox couple, and ApB was then released by hydrolysis with V8 protease, followed by the final purification to homogeneity by reverse-phase HPLC on a C4 column (*29*). Molecular weights of purified toxins were then confirmed by MALDI-TOF MS (Matrix-assisted laser desorption ionization−time-of-flight mass spectrometry) analysis on a Bruker (Billerica, MA) Biflex IV spectrometer. For some of the pKB13 derived toxins, a second polypeptide having a single glutamyl N-terminal extension was also present in variable yield. Cleavage of pJL2-derived proteins with V8 protease yields a form of ApB having an additional methionine residue at its amino terminus. We have previously shown that the glutamyl extension has no effect on toxin affinity (*26*), nor does a two residue Gly-Arg extension (*29*). Therefore, mixtures of the 49- and 50-residue products were used without additional fractionation. Typical recovery for homogeneous, wild-type ApB (wt-ApB) is about 1−2 mg per 4 L of culture; all mutants studied here gave similar yields.

Secondary structural contents were determined by far-UV circular dichroism (CD) spectropolarimetery on a Jasco (Easton, MD) J-710 spectropolarimeter. For CD analysis, all proteins were prepared at 20 $\mu$M in a 5 mM sodium phosphate buffer at pH 6.9. Spectra were recorded at 0.1-nm increments at a rate of 50 nm/s. Averages of four repeated spectra were smoothed and baseline-subtracted. The folding status of mutant peptides was assessed by comparing their molecular ellipticities to that of the wild-type toxin.

*Electrophysiology.* All toxin kinetics were measured by a whole-cell voltage clamp using an Axopatch 200B or 1D amplifier, a Digidata 1321 analog converter, and the Clampex 8.1 (Axon Instruments, Union City, CA) running on a Pentium-based IBM-compatible computer. Data were analog-filtered at 5 kHz and digitized at 20 kHz. Borosilicate glass pipets were pulled and polished to 1−4 M$\Omega$ resistances. The bath solution used for N1E-115 cells was composed of 70 mM NaCl, 70 mM CsCl, 2 mM $CaCl_2$, and 10 mM Hepes at pH 7.4 and titrated with CsOH. The bath solution for HEK-293 cells stably transfected with $Na_V1.5$ was the same except that the NaCl concentration was decreased to 5−10 mM and the CsCl concentration was increased accordingly to decrease the current magnitude and thereby maintain voltage control (*30*). The pipet solution for N1E-115 cells contained 90 mM CsF, 10 mM NaCl, 30 mM CsCl, 10 mM Hepes, and 10 mM EGTA at pH 7.0 titrated with CsOH. For the transfected HEK cells, the NaCl concentration was decreased to 2−5 mM and CsF concentration was increased accordingly so that the internal/external sodium ratio maintained the reversal potential for sodium. Either suction or an electrical pulse was used on cells having gigaohm seal resistances to obtain whole-cell access. All experiments were conducted at room temperature (22 °C).

Voltage control was determined by examination of the slope factor of the conductance transform, which needed to be greater than 4.7 mV. Only cells with greater than 0.5-

GΩ seal resistances were accepted. Toxin concentrations ranged from 100 nM to 2 $\mu$M, depending empirically on the toxin concentration necessary to yield ~50% modification. Stored data were leak- and capacitance-corrected using locally written Matlab program (Natick, MA) (*13*). Stored data were leak-corrected based on the resistance calculated from interpolation between the current at holding potential and 0 mV or from a linear fit to currents negative to the range of channel activation. Data were capacity-corrected using 8−16 summed subthreshold depolarizations, and these data were digitally refiltered at 5 kHz using a zero-phase fitting algorithm.

Clamped cells expressing human $Na_V1.5$ (stably transfected HEK-293 cells) were hyperpolarized to −130 mV to ensure full availability of all channels upon membrane depolarization. The voltage was stepped to −30 mV for 11 ms every 1−10 s while perfusing with a toxin-containing or toxin-free bath solution, which allowed determination of the modification and dissociation rates for all toxins tested. At this potential, currents from untreated cells decayed to baseline within 2−3 ms, while ApB modified currents decayed only very slowly. Therefore, we attributed the averaged residual current at 7−8 ms after depolarization to channel modification by ApB toxin. To compare the modification of multiple cells directly, the residual 7−8-ms current was normalized to the leak- and capacity-corrected peak current. For comparison of the dissociation kinetics, currents were normalized to the maximum residual current. We then fit the normalized current as a function of time from initiation of toxin application or wash out with an exponential function with a least-squares minimization routine using Origin 6.1 (Microcal Software, Inc., Northampton, MA). The inverse of $\tau$ from the fit was equal to the kinetic constant for the rate of toxin modification ($k_{mod}$) or dissociation ($k_{off}$), respectively. From these rates, a concentration-independent rate of toxin association was calculated using the equation $k_{on} = (k_{mod} - k_{off})/[toxin]$. The dissociation constant ($K_D$) was then calculated from the averaged dissociation and association rates (*13*). In a few cases, binding was so poor that it precluded the calculation of $K_D$ kinetically. In these cases, affinity was estimated from the extent of modification at a single toxin concentration using the Langmuir isotherm, $K_D = C(1/f_{mod} - 1)$, where $C$ is the concentration and $f_{mod}$ is the fraction of the current modified.

*Molecular Modeling.* Molecular models were constructed from the available ApB structure (PDB 1apf) (*16*) using Insight and Discover (Accelrys, San Diego, CA) on a SGI Octane computer with extreme graphics to assess the potential for steric hindrance because of amino acid replacement.

## RESULTS

*Qualitative Characterization of Mutant ApB Toxins.* Because the important contributions of the loop residues Gly-10, Arg-12, and Leu-18 to anemone toxin activity have been previously demonstrated, the present study was designed to determine the effects of mutagenesis at positions Asn-16, Thr-17, and Ser-19 of ApB to $Na_V$ channel affinity and isoform selectivity. Using a bacterial expression system, the neutral or charged mutant toxins N16A/D/R, T17A/D, and S19A/D/R were obtained. These ApB variants were characterized biochemically by molecular weight, HPLC retention time, recovery, and CD spectropolarimetry. From the first three criteria, the eight mutant proteins were homogeneous and similar to wt-ApB. The CD spectra of the variant toxins (Figure 2) showed positive ellipticities around 230 and 195 nm with negative ellipticity from 230 to 210 nm indicative of a folded, mostly $\beta$-structure. All spectra were dominated by a large negative ellipticity around 200 nm, which has been previously observed with ApB and other small polypeptide neurotoxins (*29*, *31*, *32*). Because the spectra of these mutants overlaid with that of wt-ApB, we concluded that all of the mutant toxins examined retained a secondary structure similar to that of the wild-type toxin.

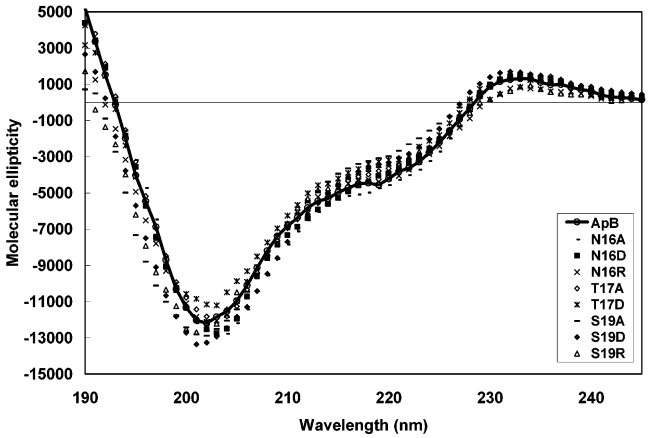


FIGURE 2: CD spectra of wt-ApB and mutant proteins. The molecular ellipticities for the mutant toxins N16A, N16D, N16R, T17A, T17D, S19A, S19D, and S19R were measured as described in the Materials and Methods. The spectra of all mutant proteins overlay with that of wild-type toxin and contain positive ellipticities at 190 and 235 nm, indicative of folded structures.

*Functional Characterization of Mutant ApB Toxins.* Our results with $Na_V1.5$ demonstrated that Thr-17 was not an important determinant of interaction with the channel. Replacement of Thr-17 with a smaller, hydrophobic side chain in T17A or with a larger, negatively charged residue in T17D had no effect on the current modification or unmodification kinetics (Table 1). When taken together with the results described below and with our previous demonstration that Leu-18 is an important binding determinant, we conclude that the side chain of Thr-17 must be oriented away from the channel.

To fully characterize the roles of Asn-16 and Ser-19 in channel binding, we created multiple substitutions at each site, including truncation of the side chain to a methyl group (N16A and S19A) and replacement by both cationic (N16/S19R) and anionic (N16/S19D) side chains. In contrast to the results seen with Thr-17, mutagenesis at Asn-16 and Ser-19 resulted in substantial changes in channel affinity, which were both substitution- and channel-isoform-dependent. At both sites, the most dramatic effects were obtained by mutation to aspartic acid, implying the existence of an important electrostatic component in the binding site. The N16D and S19D toxins were seen to bind approximately 500 and 100 times less tightly than wild-type ApB to $Na_V1.5$, respectively (Figure 3, Table 1). In both cases, the loss of affinity was dominated by increases in $k_{off}$, which was increased by 155- and 40-fold, respectively (parts B and C of Figure 4). In contrast, changes in the association rates

Table 1: Kinetic and Thermodynamic Constants for wt-ApB and Mutants on $Na_V1.5$[a]

| toxin | extent of modification (%) | $k_{on}$ ($10^5$ $M^{-1}$ $s^{-1}$)[b] | $k_{off}$ ($10^{-3}$ $s^{-1}$) | $K_D$ (nM)[c] |
|---|---|---|---|---|
| wt-ApB | 95 ± 5 | 10.9 ± 0.9 | 1.29 ± 0.27 | 1.2 |
| (100 nM) | ($n$ = 12) | ($n$ = 12) | ($n$ = 8) | |
| S19A | 78 ± 5 | 14.4 ± 4.8 | 9.8 ± 3.0 | 6.8 |
| (100 nM) | ($n$ = 5) | ($n$ = 5) | ($n$ = 5) | |
| S19R | 94 ± 7 | 3.0 ± 0.4 | 2.1 ± 0.4 | 6.8 |
| (100 nM) | ($n$ = 8) | ($n$ = 8) | ($n$ = 7) | |
| S19D | 79 ± 6 | 5.1 ± 1.3 | 52 ± 14 | 102 |
| (300 nM) | ($n$ = 6) | ($n$ = 6) | ($n$ = 6) | |
| T17A | 91 ± 6 | 12.1 ± 3.7 | 1.5 ± 0.5 | 1.2 |
| (100 nM) | ($n$ = 6) | ($n$ = 6) | ($n$ = 4) | |
| T17D | 76 ± 3 | 11.4 ± 1.7 | 3.0 ± 0.4 | 2.6 |
| (100 nM) | ($n$ = 8) | ($n$ = 5) | ($n$ = 7) | |
| N16A | 87 ± 8 | 7.3 ± 1.1 | 7.2 ± 1.4 | 9.9 |
| (100 nM) | ($n$ = 5) | ($n$ = 5) | ($n$ = 4) | |
| N16R | 74 ± 4 | 18.5 ± 1.4 | 10.3 ± 1.0 | 5.6 |
| (100 nM) | ($n$ = 4) | ($n$ = 8) | ($n$ = 7) | |
| N16D | 59 ± 3 | 3.4[d] | 219 ± 98 | 598 |
| (2000 nM) | ($n$ = 18) | | ($n$ = 4) | |

[a] Averaged kinetic rates were measured as described in the text and are shown with standard errors. [b] For $k_{on}$, if both $k_{mod}$ and $k_{off}$ were not available for one cell, the average value for the appropriate constant was used for the calculation. [c] $K_D$'s were calculated using the averaged values for $k_{off}$ and $k_{on}$. [d] For N16D, the given $k_{on}$ was calculated using the averaged $k_{mod}$ and $k_{off}$.

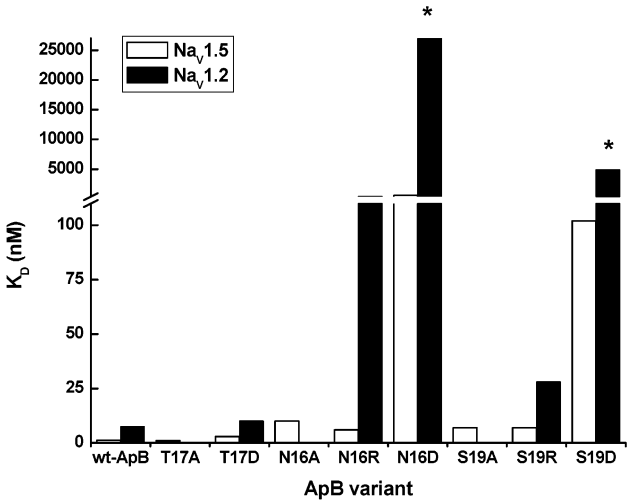


FIGURE 3: Dissociation constants of wild-type ApB and mutant toxins from $Na_V1.5$ and $Na_V1.2$. $K_D$'s for wt-ApB, T17A, T17D, N16A, N16D, N16R, S19A, S19D, and S19R for $Na_V1.5$ (open bars) were calculated from measured modification and dissociation kinetics as described in the text. For $Na_V1.2$ (filled bars), values were calculated in the same way, except for those of S19D and N16D (indicated by the asterisks), which were estimated using the Langmuir isotherm.

were 3-fold or smaller regardless of the substitution made (Figure 5). We attribute these results, particularly for the sterically conservative N16D mutation, to electrostatic repulsion between the mutant toxin and a negatively charged group or electron-dense channel region in the vicinity of site 3.

To investigate this possibility further, we also analyzed alanine and arginine replacements at each site (Table 1). While the $Na_V1.5$ affinities of the N16A, N16R, S19A, and S19R toxins were all decreased relative to the wild type (Figure 3), these losses were much less severe than those described above, ranging from 4- to 8-fold. In general, the

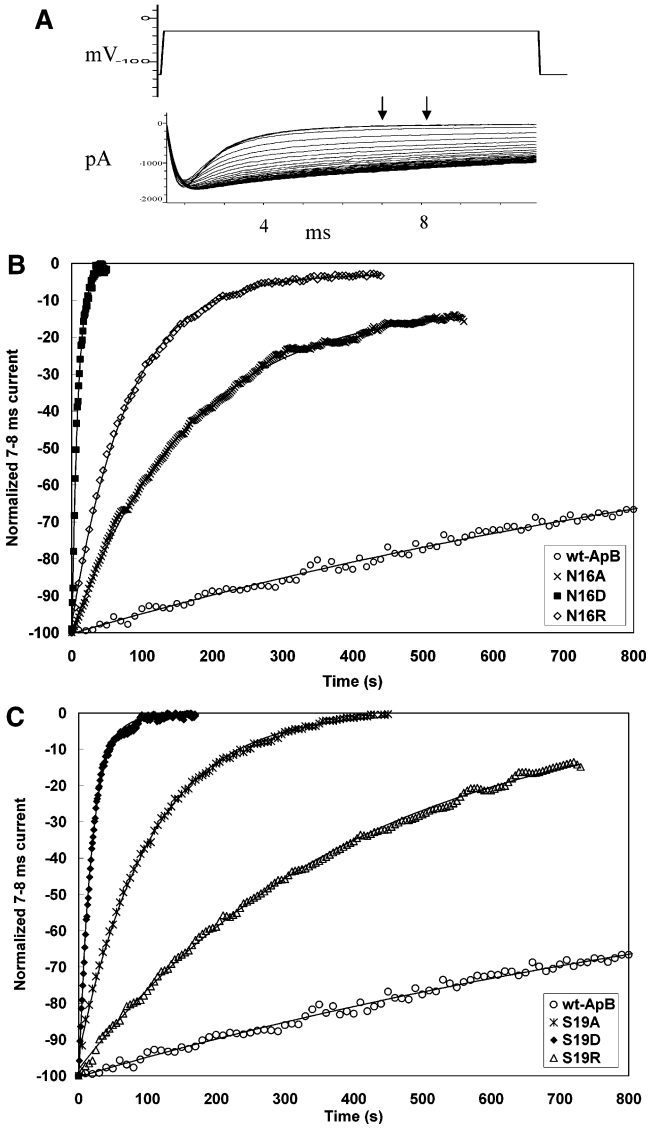


FIGURE 4: Dissociation kinetics of wild-type ApB and mutant toxins from $Na_V1.5$. (A) Representative data set with the voltage step protocol used for $Na_V1.5$ is shown with arrows marking the 7−8-ms window current used to generate the modification (B and C) and dissociation (Figure 3) curves. (B) Data points depict representative dissociation data for wt-ApB ($\tau$ = 2015 s) and the mutant proteins S19R ($\tau$ = 408 s), S19A ($\tau$ = 104.5 s), and S19D ($\tau$ = 18.9 s). Data are normalized to the peak current as described in the text. Solid lines represent fits of the data to single-exponential functions. (C) Dissociation of wt-ApB and the Asn-16 mutant proteins N16R ($\tau$ = 80 s), N16A ($\tau$ = 151.3 s), and N16D ($\tau$ = 5.0 s) is presented as described above.

alanine replacements were marginally more deleterious than the substitution to arginine. Once again, losses of affinity were dominated by changes in off rates (parts B and C of Figure 4). Although we cannot completely exclude the contribution of a steric component to these effects, or one in which indirect conformational changes play a major role, our results are fully consistent with the electrostatic interpretation given earlier for aspartate mutants.

We have previously defined the isoform discrimination index (DI) as being the ratio of the toxin dissociation constants ($K_D$) for $Na_V1.2$ and $Na_V1.5$ channels (*30*). To determine the effects of the charged mutations described above on DI, we also measured the kinetic constants of toxins mutated to arginine or aspartate at positions 16 and 19 for

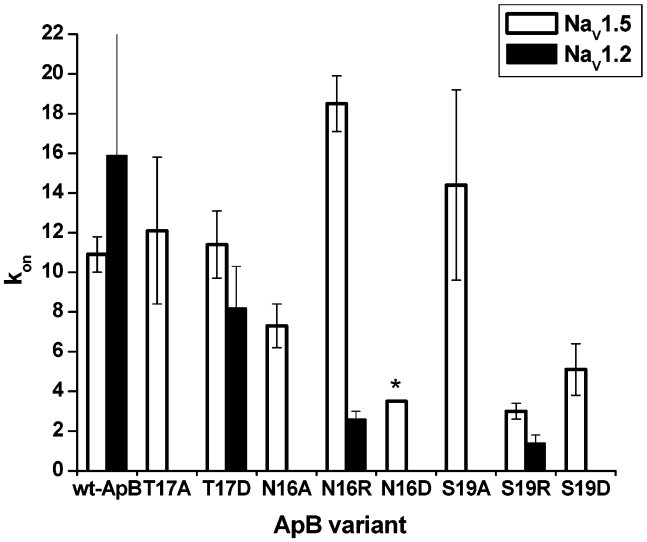


FIGURE 5: Association kinetics for wild-type ApB and mutant toxins. Association rates were calculated from modification and dissociation data obtained at toxin concentrations ranging from 0.1 to 2 $\mu$M as described in the Materials and Methods. Open bars indicate Na$_V$1.5, and filled bars indicate Na$_V$1.2. Error bars represent the standard deviations of the measurements made from 4 to 12 cells. The $k_{on}$ for N16D toxin (asterisk) was calculated from the averaged rates of modification and dissociation.

Table 2: Kinetic and Thermodynamic Constants for wt-ApB and Mutants on Na$_V$1.2[a]

| toxin | extent of modification (%) | $k_{on}$ ($10^5$ M$^{-1}$ s$^{-1}$)[b] | $k_{off}$ ($10^{-3}$ s$^{-1}$) | $K_D$ (nM)[c] | DI[d] |
|---|---|---|---|---|---|
| ApB (100 nM) | 45 ± 2 ($n$ = 6) | 15.9 ± 7.7 ($n$ = 5) | 12.0 ± 1.4 ($n$ = 9) | 7.5 | 6 |
| S19R (500 nM) | 37 ± 6 ($n$ = 6) | 1.4 ± 0.4 ($n$ = 6) | 29 ± 9 ($n$ = 6) | 204 | 30 |
| S19D (2000 nM) | 29 ± 6 ($n$ = 6) | na[e] | na | 4900 | 48 |
| T17D (500 nM) | 46 ± 8 ($n$ = 4) | 8.2 ± 2.1 ($n$ = 4) | 25 ± 9 ($n$ = 3) | 31 | 12 |
| N16R (500 nM) | 51 ± 4 ($n$ = 4) | 2.6 ± 0.4 ($n$ = 6) | 109 ± 16 ($n$ = 6) | 421 | 75 |
| N16D (2000 nM) | 7 ± 4 ($n$ = 2) | na | na | 27 000 | 45 |

[a] Averaged kinetic rates were measured as described in the text and are shown with standard errors. [b] For $k_{on}$, if both $k_{mod}$ and $k_{off}$ were not available for one cell, the average value for the missing constant was used for the calculation. [c] $K_D$'s were calculated using the averaged values for $k_{off}$ and $k_{on}$, except for S19D and N16D, which were calculated using the Langmuir Isotherm. [d] DIs, calculated as the ratio of the $K_D$ of Na$_V$1.2 over the $K_D$ of Na$_V$1.5, are also provided. [e] na = not available.

murine Na$_V$1.2 expressed in the neuroblastoma cell line N1E-115. Procedures and measurements were the same for Na$_V$1.5 except that the depolarizing voltage step was increased to −10 mV, because these channels activate at more positive voltages. To compensate for the lower level of channel expression in these cells, bath solutions contained 70 mM $Na^+$. Wild-type toxin exhibited an approximately 5-fold lower affinity to Na$_V$1.2 than to Na$_V$1.5 (Figure 3). This decrease was due exclusively to an increased dissociation rate (Tables 1 and 2). As with Na$_V$1.5, T17D displayed kinetics similar to the wild-type toxin for Na$_V$1.2; therefore, its DI was also comparable (Table 2).

Consistent with the results obtained for Na$_V$1.5, binding to Na$_V$1.2 was affected most severely by mutation of either

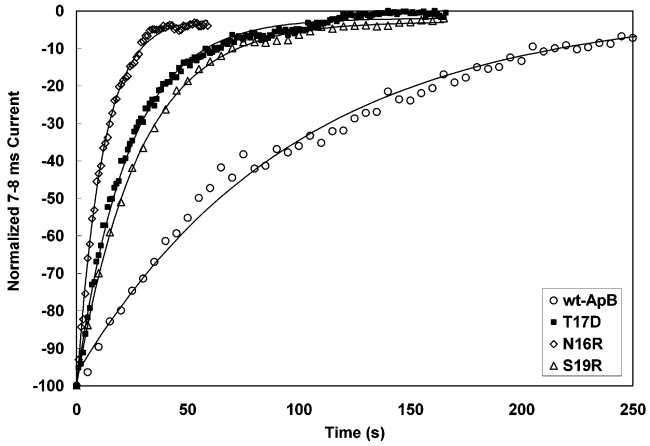


FIGURE 6: Dissociation kinetics of wild-type ApB and mutant toxins from Na$_V$1.2. Representative dissociation data for wt-ApB ($\tau$ = 97.9 s), S19R ($\tau$ = 27.8 s), N16R ($\tau$ = 11.6 s), and T17D ($\tau$ = 23.4 s) are indicated by the data points. Data are normalized to the peak current as described in the text. Solid lines represent fits of the data to single-exponential functions.

toxin site to aspartic acid, although the affinity phenotypes of both the arginine and aspartate replacements were more severe on the neuronal channel (Table 2). This exacerbated loss of affinity arose from a combination of decreased association rates as well as increased off rates for the N16R and S19R mutants, both of which associated to Na$_V$1.2 approximately 10 times more slowly than did wild-type ApB (Figure 5). Moreover, both toxins dissociated more rapidly (Figure 6, Table 2), with N16R being more severely impaired in this respect.

In contrast, the Na$_V$1.2 affinities of both N16D and S19D toxins were so severely impaired that they precluded an accurate estimation of their association rates. Even at 2 $\mu$M toxin, the extent of modification by N16D was only about 10% above the background level. Because of this, we chose to estimate the $K_D$'s for N16D and S19D by substituting the maximum extent of modification observed with either toxin into the Langmuir equation. This approach allowed us to estimate a dissociation constant for N16D of 27 $\mu$M (Figure 3, Table 2). However, because the applied toxin concentration was only 10% of this approximated $K_D$ and measurements above the background could only be made on two cells, this number must be interpreted very cautiously. Nonetheless, such a dramatically increased $K_D$ was consistent with both the greatly decreased affinity of N16D toxin for Na$_V$1.5 and with the generally lower affinity of all ApB variants for Na$_V$1.2. The same approach was also used to estimate the dissociation constant for S19D as being 5 $\mu$M (Figure 3) based upon the extent of modification observed at 2 $\mu$M toxin (29%, Table 2). DIs for all four of these mutant toxins were therefore increased (Table 2), that is, each mutant displayed a greater selectivity for Na$_V$1.5 relative to Na$_V$1.2. The DI of wild-type ApB was approximately 6, whereas this value was 30−75 in the mutant toxins analyzed here. No obvious relationship was observed between the nature or position of a given substitution and its quantitative effect on DI.

## DISCUSSION

We have previously demonstrated that residues in or flanking the Arg-14 loop of ApB make important contributions to toxin binding to site 3. In particular, Arg-12 is a

key determinant of channel-isoform selectivity (*29*, *30*), and even very conservative replacements for Leu-18 (*23*) decrease binding by over 2 orders of magnitude. Furthermore, replacement of Gly-10 or Gly-15 by alanine also decreases the binding affinity substantially, an effect that we have attributed to the restriction of conformational freedom within the Arg-14 loop (*21*). The results of the present study highlight the importance of electrostatic interactions within and near the C-terminal end of this loop and raise important implications regarding channel residues contributing to site 3.

Our most important findings are (1) that key toxin binding determinants exist within and proximal to the C terminus of the Arg-14 loop of ApB, and that this region is most likely in close contact with the channel; (2) that although electrostatic attractions between this region of the wild-type toxin and the channel cannot be essential for binding, the channel region, which contacts the Arg-14 loop (i.e., site 3) must contain either anionic residues or those having electron-rich side chains; and (3) that Thr-17, uniquely among residues 16−19, has its side chain oriented away from the channel in the binary complex.

It is obvious that the effects of mutagenesis of Asn-16 and Ser-19 of ApB are both charge- and channel-isoform-dependent and that the most deleterious substitution tested at either position was to an aspartic acid residue. In the case of the isosteric replacement N16D, the most likely explanation for this loss of affinity is by far electrostatic repulsion. However, because this portion of the wild-type toxin is uncharged, electrostatics involving fixed charges cannot be an important determinant of binding. Nonetheless, the fact that the introduction of negative charges at either position greatly increases toxin off rates strongly supports the concept of a region of high electron density in at least a portion of site 3. This electron density could result from the presence of residues having anionic side chains or from a relative abundance of aromatic residues, each with an electron-dense $\pi$ cloud.

If the former explanation were true, it should be possible to define a partner by mutant cycle analysis. We therefore expressed the isosteric neutralizing channel mutants E1548Q, D1550N, D1551N, E1555Q, E1685Q, D1689N, D1690N, D1714N, and D1729N in HEK293 cells and tested each for restoration of high-affinity binding of N16D toxin. Each mutated channel-bound N16D with an affinity comparable to that of wild-type $Na_V1.5$ (Seibert et al., unpublished). Moreover, Rogers et al. were unable to demonstrate any effect on *Leiurus* toxin binding to $Na_V1.2$ channels upon mutation of any of the remaining putatively extracellular carboxylates of domain IV (*14*). Thus, $Na_V1.2$ E1613 and the corresponding $Na_V1.5$ D1612 remain the only channel carboxylates that have been directly demonstrated to interact with bound site 3 toxins. Although the location of such carboxyl groups may need to be reexamined in view of recently proposed models describing the structure of voltage-sensitive cation channels (*34*, *35*), these results tend to favor the second explanation above. Electrostatic attractions between $\pi$ clouds and cationic side chains have been documented in many systems, including the interaction of tetrodotoxin with cardiac sodium channels (*35*−*37*).

As already noted, electrostatic repulsion can also explain the greatly increased off rate from $Na_V1.5$ observed for S19D toxin, with only a very modest change for S19R. Once again, the putative channel residue involved in this effect is unidentified. However, the known flexibility of this region of anemone toxins, when taken together with the significant conformational changes undergone by the channel, raises the interesting possibility that the same channel residue(s) drives repulsion of both the N16D and S19D toxins. Whether or not this is true, the fact that both positively and negatively charged substituents decrease affinity would seem to rule out simple point to point electrostatic repulsion as being wholly responsible.

In the majority of cases in which binding of mutated toxins to channels is measured, off rates are most severely impacted; only in rare cases are there significant effects upon rates of channel modification. This pattern is consistent with the one we observe here. Moreover, because of the inherently flexible nature of both the ligand and the acceptor molecule, it is at best very difficult to make predictive correlations between changes in on and off rates. Such correlations must assume that the binding interaction surfaces remain constant, and it is well-established that the region of the sodium channel to which site 3 toxins bind undergoes a substantial conformational change under the conditions in which we assay binding and dissociation.

The effects of the N16D and S19D mutations on $Na_V1.2$ are even more severe. As a result, the N16D/R and S19D/R toxins display enhanced selectivity for $Na_V1.5$ at the expense of binding to $Na_V1.2$. These differences in toxin-binding kinetics to the two channel isoforms suggest that the ApB-binding sites on the $Na_V1.2$ and $Na_V1.5$ channels are not identical, a conclusion which is consistent with other recent results from our laboratories (*21*), indicating that site 3 of $Na_V1.2$ is less accommodating than that of $Na_V1.5$.

It is also possible that the increased $K_D$'s for N16D and S19D are due to altered intramolecular interactions. Very few through space distance restraints have been observed for residues 8−17 in any anemone toxin, and it is therefore possible that a residue within this flexible loop could interact with Asn-16 or Ser-19 (e.g., through a hydrogen bond). Although a single interaction would be unlikely to fully stabilize any particular structure throughout the loop, its formation and breakdown could nonetheless influence the loop orientation via a propagated structural effect, i.e., transient formation of such a bond could restrict the toxin to a high- or low-affinity conformation. Clearly, such effects could also be channel-isoform-dependent. To assess the likelihood of intramolecular electrostatics, the proximity of other charged residues of ApB to Asn-16 was assessed by molecular modeling. The most likely suspects, because of their presence in the Arg-14 loop, are Asp-9, Arg-12, and Arg-14. Neither the nearest acidic side chain, Asp-9, nor the guanidinium groups of Arg-12 or Arg-14 approach closely enough to interact with either Asn-16 or Ser-19 in any of the 20 calculated structures (16). In none of these pairs does the sides chains approach closer than an averaged 10 Å. Even so, loop conformational dynamics could be affected by an interaction (e.g., between N16D and an undefined toxin residue). A subset of the ApB structures calculated by Monks et al. (*16*) suggested the presence of a type II $\beta$ turn stabilized by a hydrogen bond between the backbone carbonyl of Pro-13 and the backbone amide group of Asn-16. Chou−Fasman analysis predicts similar turn probabilities for the sequences

PRGN (wt-ApB) and PRGD (N16D), but it remains possible that the stability of this turn is changed in N16D.

In conclusion, charge-dependent alterations in kinetics occur upon substitution at Asn-16 or Ser-19. These residues are highly conserved throughout the type 1 sea anemone toxin family, while Thr-17, which is not important for ApB affinity to $Na_V$ channels, is not. At either position, replacement by an anionic residue yields the most severe phenotype, perhaps indicating the presence of electron-dense side chains within site 3. When taken together with previous work from our laboratory (*21*−*23*), the present data suggest that the "flexible" loop region encompassing residues 8−17, together with the adjacent C-terminal residues Leu-18 and Ser-19, are critical determinants of the tight channel affinity of ApB as well as contributing to the preference for $Na_V1.5$ displayed by this toxin.

## ACKNOWLEDGMENT

The ApB expression plasmids pJL2 and pJL5 were constructed by June Liu, pSA2 by Sujith Alphy, and plasmids expressing mutated $Na_V1.5$ by Al Combs. We thank Dana McLymond and Sujith Alphy for their assistance with mutagenesis and protein purification, Connie Mlecko for her assistance with cell-culture maintenance, Megan McNulty, Dr. Tom Suchyna, and Dr. Sergio Elenes for their guidance with the Buffalo electrophysiology setup, and Dr. Tony Auerbach for the use of his pipet puller and polisher.

## REFERENCES

1. Norton, R. S. (1991) Structure and structure−function relationships of sea anemone proteins that interact with the sodium channel, *Toxicon 29*, 1051−1084.
2. Catterall, W. A., and Beress, L. (1978) Sea anemone toxn and scorpion toxin share a common receptor site associated with the action potential sodium ionophore, *J. Biol. Chem. 253*, 7393−7396.
3. Catterall, W. A. (1988) Structure and function of voltage-sensitive ion channels, *Science 242*, 50−61.
4. Catterall, W. A. (1992) Cellular and molecular biology of voltage-gated sodium channels, *Physiol. Rev. 72*, S15−S47.
5. Cestele, S., and Catterall, W. A. (2000) Molecular mechanisms of neurotoxin action on voltage-gated sodium channels, *Biochimie 82*, 883−892.
6. Blumenthal, K. M., and Seibert, A. L. (2003) Voltage-gated sodium channel toxins: poisons, probes, and future promise, *Cell Biochem. Biophys. 32*, 215−238.
7. Pallaghy, P. K., Scanlon, M. J., Monks, S. A., and Norton, R. S. (1992) Three-dimensional structure in solution of the polypeptide cardiac stimulant Anthopleurin-A, *Biochemistry 34*, 3782−3794.
8. Landon, C., Sodano, P., Cornet, B., Bonmatin, J. M., Kopeyan, C., Rochat, H., Vovelle, F., and Ptak, M. (1997) Refined solution structure of the anti-mammal and anti-insect LqqIII scorpion toxin: Comparison with other scorpion toxins, *Proteins 28*, 360−374.
9. Hanck, D. A., and Sheets, M. F. (1995) Modification of inactivation in cardiac sodium channels: Ionic current studies with Anthopleurin-A toxin, *J. Gen. Physiol. 106*, 601−616.
10. Sheets, M. F., and Hanck, D. A. (1995) Voltage-dependent open-state inactivation of cardiac sodium channels: Gating current studies with Anthopleurin-A toxin, *J. Gen. Physiol. 106*, 617−640.
11. Sheets, M. F., and Hanck, D. A. (1999) Gating of skeletal and cardiac muscle sodium channels in mammalian cells, *J. Physiol. 514*, 425−436.
12. Sheets, M. F., Kyle, J. W., Kallen, R. G., and Hanck, D. A. (1999) The Na channel voltage sensor associated with inactivation is localized to the external charged residues of domain IV, S4, *Biophys. J. 77*, 747−757.
13. Benzinger, G. R., Kyle, J. W., Blumenthal, K. M., and Hanck, D. A. (1998) A specific interaction between the cardiac sodium channel and site-3 toxin Anthopleruin B, *J. Biol. Chem. 273*, 80−84.
14. Rogers, J. C., Qu, Y., Tanada, N., Scheuer, T., and Catterall, W. A. (1996) Molecular determinants of high affinity binding of α-scorpion toxin and sea anemone toxin in the S3−S4 extracellular loop in domain IV of the sodium channel α subunit, *J. Biol. Chem. 271*, 15950−15962.
15. Lehmann-Horn, F., and Jurkat-Rott, K. (1999) Voltage-gated ion channels and hereditary disease, *Physiol. Rev. 79*, 1317−1372.
16. Monks, S. A., Pallaghy, P. K., Scanlon, M. J., and Norton, R. S. (1995) Solution structure of the cardiostimulant polypeptide Anthopleurin-B and comparison with Anthopleurin-A, *Structure 3*, 791−803.
17. Torres, A. M., Bansal, P., Alewood, P. F., Bursill, J. A., Kuchel, P. W., and Vandenberg, J. I. (2003) Solution structure of CnErg1 (Ergtoxin), a HERG specific scorpion toxin, *FEBS Lett. 539*, 138−142.
18. Takeuchi, K., Park, E., Lee, C., Kim, J., Takahashi, H., Swartz, K., and Shimada, I. (2002) Solution structure of ω-grammotoxin SIA, a gating modifier of P/Q and N-type $Ca^{2+}$ channel, *J. Mol. Biol. 321*, 517−526.
19. Kohno, T., Sasaki, T., Kobayashi, K., Fainzilber, M., and Sato, K. (2002) Three-dimensional solution structure of the sodium channel agonist/antagonist δ-conotoxin TxVIA, *J. Biol. Chem. 277*, 36387−36391.
20. Fogh, R. H., Kem, W. R., and Norton, R. S. (1990) Solution structure of Neurotoxin I from the sea anemone *Stichodactyla helianthus*, *J. Biol. Chem. 265*, 13016−13028.
21. Seibert, A. L., Lui, J. R., Hanck, D. A., and Blumenthal, K. M. (2003) Arg-14 loop of site 3 anemone toxins: Effects of glycine replacement on toxin affinity, *Biochemistry 42*, 14515−14521.
22. Gallagher, M. J., and Blumenthal, K. M. (1994) Importance of the unique cationic residues Arginine 12 and Lysine 49 in the activity of the cardiotonic polypeptide Anthopleurin B, *J. Biol. Chem. 269*, 254−259.
23. Dias-Kadambi, B. L., Combs, K. A., Drum, C. L., Hanck, D. A., and Blumenthal, K. M. (1996) Leucine 18, a hydrophobic residue essential for high affinity binding of Anthopleurin B to the voltage-sensitive sodium channel, *J Biol. Chem. 271*, 9422−9428.
24. Khera, P. K., and Blumenthal, K. M. (1994) Role of the Cationic Residues Arginine 14 and Lysine 48 in the Function of the Cardiotonic Polypeptide Anthopleurin B, *J. Biol. Chem. 269*, 921−925.
25. Khera, P. K., and Blumenthal, K. M. (1996) Importance of Highly Conserved Anionic Residues and Electrostatic Interactions in the Activity and Structure of the Cardiotonic Polpeptide Anthopleurin B, *Biochemistry 35*, 3503−3507.
26. Kelso, G. J., Drum, C. L., Hanck, D. A., and Blumenthal, K. M. (1996) Role of Pro-13 in directing high-affinity binding of Anthopleurin B to the voltage-sensitive sodium channel, *Biochemistry 35*, 14157−14164.
27. Hirsh, J. K., and Quandt, F. N. (1996) Down-regulation of Na channel expression by A23187 in N1E−115 neuroblastoma cells, *Brain Res. 706*, 343−46.
28. Benzinger, G. R., Tonkovich, G. S., and Hanck, D. A. (1999) Augmentation of recovery from inactivation by site-3 Na channel toxins: A single-channel and whole-cell study of persistent currents, *J. Gen. Physiol. 113*, 333−346.
29. Gallagher, M. J., and Blumenthal, K. M. (1992) Cloning and expression of wild-type and mutant forms of the cardiotonic polypeptide Anthopleurin B, *J. Biol. Chem. 267*, 13958−13963.
30. Khera, P. K., Benzinger, G. R., Lipkind, G., Drum, C. L., Hanck, D. A., and Blumenthal, K. M. (1995) Multiple cationic residues of Anthopleurin B that determine high affinity channel and isoform discrimination, *Biochemistry 34*, 8533−8541.
31. Maggio, F., and King, G. F. (2002) Scanning mutagenesis of a Janus-faced atracotoxin reveals a bipartite surface patch that is essential for neurotoxic function, *J. Biol. Chem. 277*, 22806−22813.
32. Sun, Y. M., Bosmans, F., Zhu, R. H., Goudet, C., Xiong, Y. M., Tytgat, J., and Wang, D. C. (2003) Importance of the conserved aromatic residues in the scorpion α-like toxin BmK M1, *J. Biol. Chem. 278*, 24125−24131.

33. Gallivan, J. P., and Dougherty, D. A. (1999) Cation−$\pi$ interactions in structural biology, *Proc. Nat. Acad. Sci. U.S.A. 96, 9459−9464.*
34. Jiang, Y., Lee, A., Chen, J., Ruta, V., Cadene, M., Chait, B. T., and MacKinnon, R. (2003) X-ray structure of a voltage-dependent $K^+$ channel, *Nature 423*, 33−41.
35. Jiang, Y., Ruta, V., Chen, J., Lee, A., and MacKinnon, R. (2003) The principle of gating charge movement in a voltage-dependent $K^+$ channel, *Nature 423*, 42−48.
36. Dougherty, D. A. (1996) Cation−$\pi$ interactions in chemistry and biology: A new view of benzene, Phe, Tyr, and Trp, *Science 271*, 163−168.
37. Satin, J., Kyle, J. W., Chen, M., Bell, P., Cribbs, L. L., Fozzard, H. A., and Rogart, R. B. A mutant of TTX-resistant cardiac sodium channels with TTX-sensitive properties, *Science 256*, 1202−1205.

BI0496135